VISCOUS PROFILES AND NUMERICAL METHODS FOR SHOCK WAVES

Edited by Michael Shearer
North Carolina State University

siam.
Philadelphia
Society for Industrial and Applied Mathematics

VISCOUS PROFILES AND NUMERICAL METHODS FOR SHOCK WAVES

Proceedings of a workshop at North Carolina State University, Raleigh, North Carolina, May 23-25, 1990. This workshop was supported in part by the US Army Research Office Grant No. DAAL03-90-G-0011.

Library of Congress Cataloging-in-Publication Data

Viscous profiles and numerical methods for shock waves/ [edited by] Michael Shearer.
p. cm.
Proceedings of a workshop at North Carolina State University, Raleigh, North Carolina, May 23-35, 1990.
Includes bibliographical references.
ISBN 0-89871-283-1
1. Shock waves—Congresses. 2. Viscous flow—Congresses. 3. Differential equations, Hyperbolic—Numerical solutions—-Congresses. 4. Differential equations, Parabolic—Numerical solutions—Congresses. I. Shearer, Michael.
QA927.V57 1992
531'.1133—dc20 91-40934

All rights reserved. Printed in the United States of America. No part of this book may be reproduced, stored or transmitted without the written permission of the Publisher. For information, write the Society for Industrial and Applied Mathematics, 3600 University City Science Center, Philadelphia, PA 19104-2688.

Copyright © 1991 by the Society for Industrial and Applied Mathematics.

CONTENTS

Fully-Discrete Methods with Grid Refinement for the Generalized Korteweg-de Vries Equation[1]

Jerry L. Bona†
Vassilios A. Dougalis*
Ohannes A. Karakashian‡
William R. McKinney**

Abstract. A class of fully-discrete schemes for the numerical solution of the periodic initial-value problem for the generalized Korteweg-de Vries equation are presented and tested. These numerical approximations are generated by a Galerkin Finite Element process for the spatial discretization and Implicit Runge-Kutta methods for the temporal discretization. Such schemes possess excellent stability properties, as well as arbitrarily high order rates of convergence in both the spatial and temporal variables. These methods are used with adaptive grid refinement in the spatial and temporal meshes to investigate the stability and instability of a class of travelling-wave solutions known as solitary-waves. The numerical approximations give evidence that solutions of the GKdV equation can develop singularities in finite time.

1. Introduction. In this paper, numerical methods used to generate fully-discrete approximations for the generalized Korteweg-de Vries (GKdV) equation are presented. The GKdV equation is a model used to describe the propagation of nonlinear, dispersive waves and can be written in the form

$$u_t + u^p u_x + \epsilon u_{xxx} = 0, \tag{1.1a}$$

where p is a nonnegative integer and ϵ is a nonzero parameter. Here, the equation is considered with periodic boundary conditions on the spatial interval $x \in [0,1]$ and for

[1] Work supported in part by the Institute of Applied and Computational Mathematics of the Research Center of Crete, Iraklion, Crete, Greece, the National Science Foundation, USA, the Air Force Office for Scientific Research under grant AFOSR-88-0019, and the Science Alliance, University of Tennessee.

†Department of Mathematics and Applied Research Laboratory, The Pennsylvania State University, University Park, PA 16802.
*Department of Mathematics, University of Crete, Iraklion, Crete, Greece.
‡ Department of Mathematics, University of Tennessee, Knoxville, TN 37996.
**Department of Mathematics, North Carolina State University, Raleigh, NC 27695.

finite time intervals $t \in [0, t^*]$, with initial data

$$u(x,0) = u^0(x) \tag{1.1b}$$

where u^0 is a given periodic function of period 1. The value of the solution $u(x,t)$ represents the amplitude of a periodic wave at a point x at time t. The special case $p = 1$ corresponds to the well-known Korteweg-de Vries (KdV) equation.

The global existence of solutions for (1.1), with arbitrary p and large, smooth initial data u^0, is still an open question. Kato [1] has shown that if $p < 4$, then the pure initial-value problem for (1.1), wherein u^0 is specified for all x and need not be periodic, does indeed have solutions that exist for all $t > 0$, provided u^0 is sufficiently smooth and decays at infinity. A similar result holds for the periodic case (see for example [2] in the case $p = 1$). To investigate numerically the question of global existence, we shall use the family of solitary-wave solutions. A recent theory [3] has shown that these special travelling-wave solutions are stable if and only if $p < 4$. However, the theory leaves completely open the manifestation of instability. The numerical simulations given herein indicate that the instability leads to the formation of singularities in finite time.

In Section 2, the numerical schemes used to produce fully-discrete approximations to solutions of the periodic initial-value problem for the GKdV equation are presented. These schemes are a combination of a Galerkin method and Implicit Runge-Kutta methods. In this paper, only a brief description of these methods is given. A more detailed description of these schemes, including proofs of stability and convergence along with an algorithm for their efficient implementation, may be found in [4]; for earlier work and results, including a list of numerical techniques for the KdV equation, see [5] and the references therein. An important consequence of the methods used here is that they preserve the second invariant of the GKdV equation.

In Section 3, these numerical methods are used with uniform spatial and temporal meshes to simulate the solitary-wave for $p = 5$. With small initial data, the schemes are very effective. However, for larger u^0, it becomes very evident that these methods need modification. This is done in Section 4 where we introduce schemes to refine both the spatial and temporal grids. This adaptive grid algorithm is based on the third invariant of the GKdV equation and a standard inverse property of the finite elements utilized in our scheme.

2. Numerical Approximations. After introducing some basic notation, the numerical schemes used to generate the fully-discrete approximations are described. These approximations are obtained by a Galerkin Finite Element process for the spatial discretization and conservative Implicit Runge-Kutta (IRK) methods for the time-stepping. These schemes possess excellent stability properties, as well as arbitrarily high order rates of convergence in both the spatial and temporal variable. Thus, they represent an efficient means for highly accurate numerical simulations of solutions of (1.1).

For nonnegative integers m and real p, $1 \le p \le \infty$, let $W^{m,p} = W^{m,p}(0,1)$ denote the usual Sobolev spaces with norm $\|\cdot\|_{m,p}$ consisting of functions whose first m derivatives belong to L^p. For $p = 2$, note that $W^{m,2}$ is the Hilbert space H^m and replace $\|\cdot\|_{m,2}$ with $\|\cdot\|_m$. If in addition $m = 0$, we shall replace $\|\cdot\|_0$ with $\|\cdot\|$, and note that $H^0 = L^2$ with the inner product $(\cdot,\cdot)$.

2.1 Finite Element Spaces. Let r and N be integers with $3 \le r \le N$ and define $h = 1/N$. Let S_h^r denote the space of 1-periodic smooth splines of order r (polynomials of degree less than or equal to $r-1$) defined on a uniform partition of $[0,1]$, $x_i = ih$, $i = 0, \ldots, N$.

It is well-known that if v is a sufficiently smooth periodic function with period 1, then there exists a $\chi \in S_h^r$ such that for $1 \le m \le r$,

$$\sum_{j=0}^{m-1} h^j \|v - \chi\|_{j,s} \le ch^m \|v\|_{m,s}, \quad s = 2 \quad \text{or} \quad s = \infty, \tag{2.1}$$

where c is a constant independent of h, v and χ. In addition to the above *approximation* properties, the finite-dimensional spaces S_h^r also possess the following *inverse* properties. There exists a constant c, independent of h, such that for all $\chi \in S_h^r$,

$$\|\chi\|_\beta \le ch^{-(\beta-\alpha)} \|\chi\|_\alpha \quad \text{and} \quad \|\chi\|_{\alpha,\infty} \le ch^{-(\alpha+\frac{1}{2})} \|\chi\|, \tag{2.2}$$

where $0 \le \alpha \le \beta \le r-1$.

The Galerkin semidiscrete approximation to the solution u(x,t) of (1.1) is defined as a mapping $v_h : [0, t^*] \to S_h^r$ satisfying the relations

$$(v_{ht}, \chi) - (\frac{1}{p+1} v_h^{p+1} + \epsilon v_{hxx}, \chi') = 0, \quad \forall \chi \in S_h^r, \tag{2.3}$$

and

$$v_h(0) = \pi_h u^0, \tag{2.4}$$

where $\pi_h u^0$ denotes any conveniently chosen element of S_h^r (e.g. L^2-projection, interpolant, etc.) such that

$$\|\pi_h u^0 - u^0\| \le ch^r. \tag{2.5}$$

One may then show that if $u(x,t)$ is sufficiently smooth, then v_h exists uniquely and satisfies the error estimate

$$\max_{0 \le t \le t^*} \|v_h(t) - u(\cdot, t)\| \le ch^r \tag{2.6}$$

where c is a constant independent of h. (See [6] for a proof in the special case $p = 1$ which may easily be extended to larger p). Furthermore, letting $\chi = v_h$ in (2.3), integrating by parts and using periodicity, it is easy to see that

$$\|v_h(t)\| = \|v_h(0)\|, \quad t \ge 0. \tag{2.7}$$

Upon choosing a basis for S_h^r and representing v_h in terms of this basis, (2.3) then becomes a system of N nonlinear ordinary differential equations which is conservative in L^2 by (2.7).

2.2 Implicit Runge-Kutta Methods. To obtain the fully-discrete approximations, we shall discretize the system (2.3) in time by Implicit Runge-Kutta methods. (For details and general remarks concerning Runge-Kutta methods, we refer to [7] and the references therein). For positive integer q, a q-stage IRK method is given as a set of constants arranged in *tableau* form

$$\begin{array}{c|ccc} a_{11} & \cdots & a_{1q} & \tau_1 \\ \vdots & & \vdots & \vdots \\ a_{q1} & \cdots & a_{qq} & \tau_q \\ \hline b_1 & \cdots & b_q & \end{array} .$$

Of particular interest is the family of Gauss-Legendre methods. These methods are appropriate for several reasons. First, they are conservative, a property that is necessary for the existence of a discrete conservation law similar to (2.7). They are algebraically stable, a property that is much stronger than A-stability. Also, this family is optimal in that for a given q, they are the unique Runge-Kutta method of order $2q$ in the context of the approximation of solutions of systems of ordinary differential equations. The tableau for the 2-stage Gauss-Legendre method is given by

$$\begin{array}{cc|c} \frac{1}{4} & \frac{1}{4}-\frac{1}{2\sqrt{3}} & \frac{1}{2}-\frac{1}{2\sqrt{3}} \\ \frac{1}{4}+\frac{1}{2\sqrt{3}} & \frac{1}{4} & \frac{1}{2}+\frac{1}{2\sqrt{3}} \\ \hline \frac{1}{2} & \frac{1}{2} & \end{array},$$

and the tableau for the 3-stage method is

$$\begin{array}{ccc|c} \frac{5}{36} & \frac{80-24\sqrt{15}}{360} & \frac{50-12\sqrt{15}}{360} & \frac{1}{2}-\frac{\sqrt{15}}{10} \\ \frac{50+15\sqrt{15}}{360} & \frac{2}{9} & \frac{50-15\sqrt{15}}{360} & \frac{1}{2} \\ \frac{50+12\sqrt{15}}{360} & \frac{80+24\sqrt{15}}{360} & \frac{5}{36} & \frac{1}{2}+\frac{\sqrt{15}}{10} \\ \hline \frac{5}{18} & \frac{8}{18} & \frac{5}{18} & \end{array}.$$

The fully-discrete approximations are now obtained by applying a q-stage Gauss-Legendre method to the system (2.3). For integer $J > 0$, let $t^n = nk$, $n = 0, 1, \ldots, J$, where the step size is given by $k = t^*/J$. With $u(x,t)$ being the true solution of (1.1), approximations $u_h^n \in S_h^r$ to $u(\cdot, t^n)$, for $n = 0, 1, \ldots, J$ are defined by letting $u_h^0 = \pi_h u^o$, and for $n = 0, 1, \ldots, J-1$,

$$(2.8) \qquad (u_h^{n+1}, \chi) = (u_h^n, \chi) + k \sum_{i=1}^{q} b_i \left(\frac{1}{p+1}[u_h^{n,i}]^{p+1} + \epsilon u_{hxx}^{n,i}, \chi'\right), \quad \forall \chi \in S_h^r,$$

where the intermediate values $u_h^{n,i}$, $i = 1, \ldots, q$, are the solutions of the system of q nonlinear equations

$$(2.9) \qquad (u_h^{n,i}, \chi) = (u_h^n, \chi) + k \sum_{j=1}^{q} a_{ij} \left(\frac{1}{p+1}[u_h^{n,j}]^{p+1} + \epsilon u_{hxx}^{n,j}, \chi'\right), \quad \forall \chi \in S_h^r.$$

The equations (2.9) are solved by using a Newton iteration as described in [4].

2.3 Stability and Convergence. In this section we summarize results concerning the fully-discrete approximations u_h^n which can be found along with their proofs in [4]. In the following, we shall assume that $u^0(x)$ is sufficiently smooth to guarantee the existence and required smoothness of the solution $u(x,t)$ for $0 \le t \le t^*$ in order that the error estimates hold.

THEOREM 2.1. *For $n = 0, 1, \ldots, J-1$, the equations (2.8) and (2.9) have solutions $u_h^{n+1} \in S_h^r$ and $u_h^{n,i} \in S_h^r$, $i = 1, \ldots, q$. Furthermore,*

$$(2.10) \qquad \|u_h^n\| = \|\pi_h u^0\| \quad \text{for} \quad n = 0, \ldots, J.$$

The above theorem demonstrates that the fully-discrete approximations are conservative in L^2, a discrete analog of the second invariant of the GKdV.

THEOREM 2.2. *Assume that as* $h \to 0$,

(i) *if* $p = 1$, *then* $k = O(h^{\frac{3}{2(q+2)}})$ *for* $q \geq 2$ *or* $k = O(h^{\frac{3}{4}})$ *for* $q = 1$,
(ii) *if* $p = 2$, *then* $kh^{-\frac{1}{2}}$ *is sufficiently small for* $q \geq 2$ *or* $k = O(h^{\frac{3}{4}})$ *for* $q = 1$,
(iii) *if* $p \geq 3$, *then* kh^{-1} *is sufficiently small for all* $q \geq 1$.

If h *is sufficiently small, then for* $n = 0, 1, \ldots, J$, *there exists a unique solution* u_h^n *of (2.8) and (2.9) such that*

$$\max_{0 \leq n \leq J} \|u_h^n - u(\cdot, t^n)\| \leq c(k^{2q} + h^r), \quad \text{for} \quad q = 1, 2, \tag{2.11}$$

$$\max_{0 \leq n \leq J} \|u_h^n - u(\cdot, t^n)\| \leq c(k^{q+2} + h^r), \quad \text{for} \quad q \geq 3 \tag{2.12}$$

for some constant c *independent of* h *and* k.

It is worth remark that the above result is sub-optimal if $q \geq 3$. However, in the case of the KdV equation ($p = 1$), it has recently been shown [8] that the optimal temporal rate of convergence $2q$ is achieved independent of the number of stages q.

3. Numerical Simulation of Solitary Waves. In this section, the numerical schemes presented in Section 2 are tested. Specifically, we try to simulate the solitary-wave solutions of the GKdV equation. These special, travelling-wave solutions are given by

$$u(x,t) = A\, sech^{2/p}[B(x - x_0 - Ct)], \tag{3.1}$$

where

$$C = \frac{2A^p}{(p+1)(p+2)}, \quad B = \frac{p}{2}\sqrt{\frac{C}{\epsilon}}$$

and A represents the amplitude of the waves. Although (3.1) is an exact solution of the pure initial-value problem for (1.1), if A is large and ϵ is taken sufficiently small then it should also be an approximate solution in the periodic case since the tails of the solitary-wave decay exponentially.

For other numerical results regarding the order of these methods, their efficiency, and the calculation of various errors, see [4] and [5].

The numerical experiments reported here and in the next section are the results of a FORTRAN program written in double precision and run on both a SUN Sparcstation 1 and an Alliant FX/40 with identical results up to machine roundoff error.

In the following, we have used the 2-stage Gauss-Legendre method ($q = 2$) with cubic splines ($r = 4$). We also have set $p = 5$ and $x_0 = .5$ so that the wave is initially centered at $x = 1/2$. According to the theory in [3], $p = 5$ is in the range where solitary-waves are unstable.

In the first test, we took $\epsilon = 1 \cdot 10^{-4}$ and $A = .8$ as the amplitude. For spatial and temporal mesh sizes the values $h = 1/384$ and $k = 1/100$, respectively, were used. The numerical solution was computed up to $t = 18$. In Figure 1 plots of the numerical solution are given at $t = 0, t = 6, t = 12$, and $t = 18$. It is evident from the graphs that the mesh parameters used were sufficient to numerically approximate the travelling-wave solution.

Next, the size of the initial data was increased to $A = 2.0$ for the amplitude. Also, we took $\epsilon = 5 \cdot 10^{-4}$. The step size was reduced to $k = 1/5000$ and the spatial mesh remained at $h = 1/384$. Output of our code in this case are depicted in Figure 2. As can be seen from the graphs, the instability of the solitary-wave required only a small

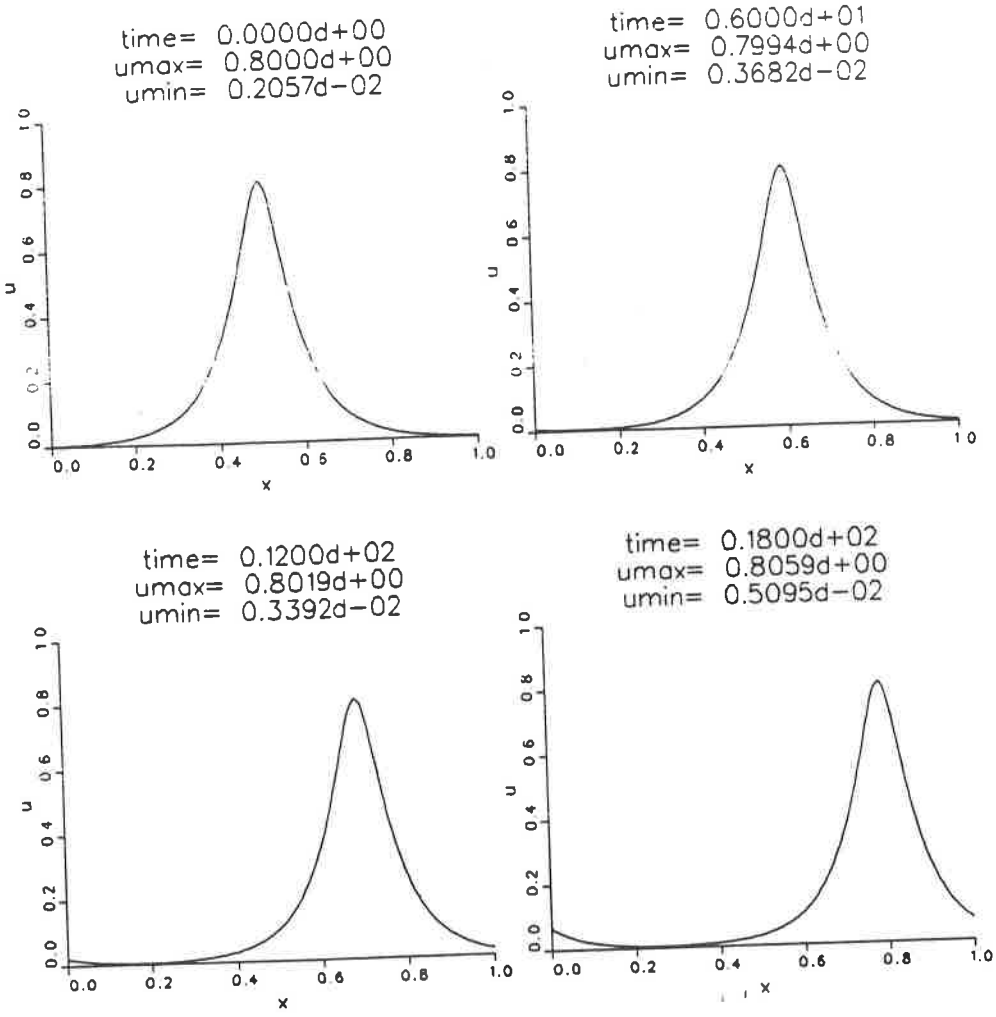

Figure 1. Numerical simulation of a solitary-wave solution with amplitude $A = 0.8$.

amount of time before it caused the numerical solution to begin to break down owing to dispersive pollution of the solution.

4. Grid Refinement. As the results of the previous section indicate, the instability of the solitary-wave solutions leads to substantial numerical errors when using fixed grids. To overcome this difficulty, an algorithm with automatic grid refinement was implemented so that one can approximate a solution $u(x,t)$ of (1.1) that develops a singularity in L^∞ at some point (x^*,t^*). The adaptive mechanism in our code consists of three main parts:

(i) local refinement of the spatial grid,
(ii) selection of a temporal step size k,
(iii) spatial translations of the solution.

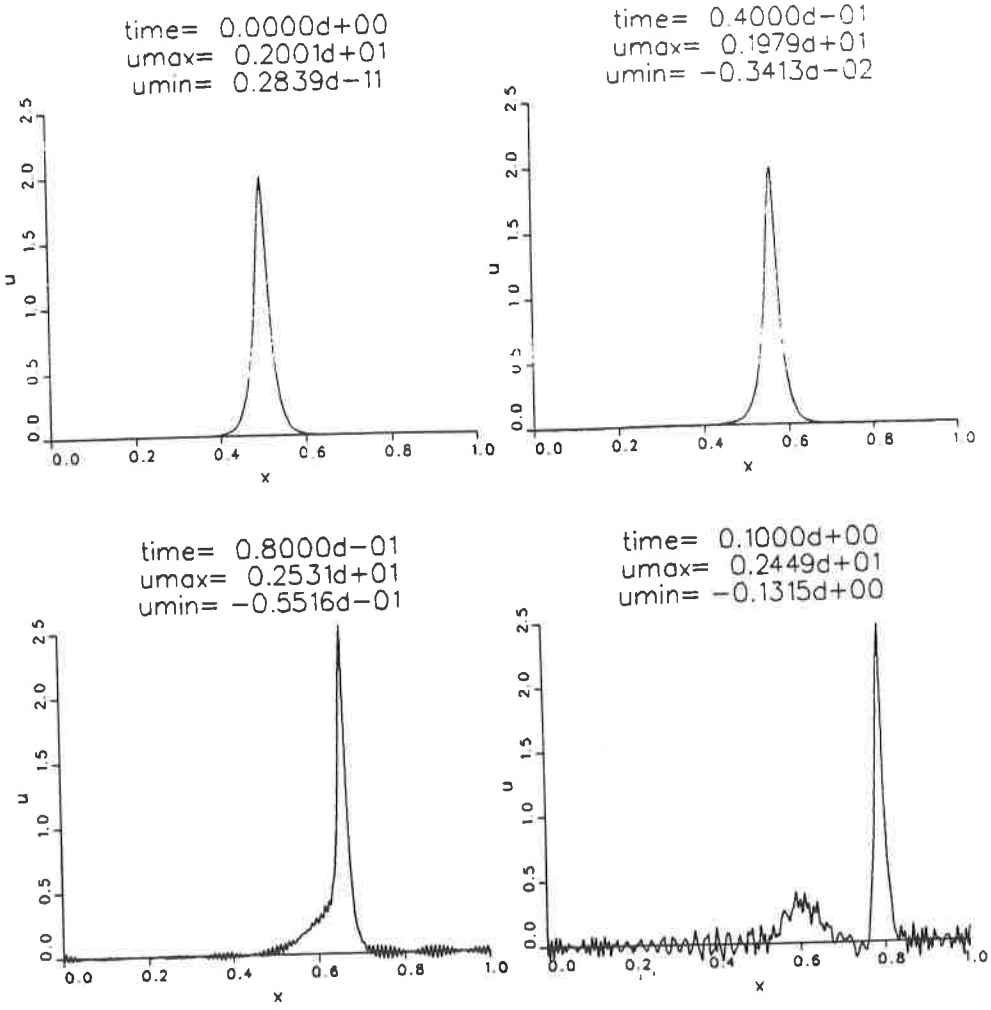

Figure 2. Numerical simulation of a solitary-wave solution with amplitude $A = 2.0$.

reak down owing

te, the instability when using fixed d refinement was) that develops a our code consists

Our spatial refinements will consist of adding new nodes, distributed evenly about the midpoint $x = .5$, but in successively smaller neighborhoods of the midpoint. This local refinement is combined with (iii), which takes advantage of the fact that the solution is a travelling-wave, to keep the peak near the midpoint $x = .5$ in the region of highest density of nodes, and away from a region of coarse mesh. This is accomplished by occasionally translating the solution and centering the peak at $x = .5$. (In effect, we translate the solution to conform to fixed grids rather than have a moving grid which conforms to the solution.)

We next describe the automatic implementation of (i).

4.1 Spatial Grid Refinement. Let *NSPLIT* stand for the number of times nodes are to be added and let Ω^* represent the neighborhood of the midpoint $x = .5$ which is

the region with the finest grid, with grid size h^*. Each time nodes are added, *NSPLIT* is increased by 1, and both Ω^* and h^* are cut in half. As an example, with *NSPLIT* = 1, we might have $\Omega^* = [0.4, 0.6]$ and $h^* = 1/100$. Then as *NSPLIT* increases to 2, $\Omega^* = [0.45, 0.55]$, $h^* = 1/200$; when *NSPLIT*= 3, $\Omega^* = [0.475, 0.525]$, $h^* = 1/400$, and so on. The effect of the occasional spatial translations is to insure that the peak of the solution remains in the region Ω^*.

From the $L^\infty - L^2$ inverse inequality in (2.2) and the discrete conservation law (2.10), it follows that for a uniform mesh

$$\|u_h^n\|_{0,\infty} \le ch^{-1/2}\|u_h^n\| = ch^{-1/2}\|\pi_h u^0\| \quad \text{for} \quad n = 0, ..., J. \tag{4.1}$$

Similarly, for a non-uniform grid the minimal grid size h^* must become arbitrarily small if the numerical solution is to develop an arbitrarily large peak. Our particular choice of spatial refinement is based on a local $L^\infty - L^2$ inverse property on Ω^*. Specifically, we use the following test to determine if *NSPLIT* needs to be increased. At each step, compute

$$Z_\infty = \|u_h^n\|_{0,\infty} \quad \text{and} \quad Z_2 = \left[\int_{\Omega^*} (u_h^n)^2\, dx\right]^{1/2}.$$

We then increase *NSPLIT* by 1, add new nodes, and modify Ω^* and h^* if

$$\frac{Z_\infty \sqrt{h^*}}{Z_2} > TOL_1. \tag{4.2}$$

Here TOL_1 must be chosen small enough in accordance with (4.1) to allow for new nodes to be added. In our program, we have used $TOL_1 = 0.2$.

We next describe (ii), the selection of a temporal step size k.

4.2 Temporal Step Size Reduction. The temporal step size is adjusted in an attempt to preserve the third invariant of the GKdV equation. This invariant is defined by

$$I_3(v) = \int_0^1 [v^{p+2} - \frac{(p+1)(p+2)\epsilon}{2}(v_x)^2]\, dx.$$

For exact solutions $u(x,t)$ of (1.1), $I_3(u(\cdot,t)) = I_3(u^0)$, independent of the value of t.

Given u_h^n, a possible u_h^{n+1} is computed using the current step size k. It is accepted if

$$\frac{|I_3(u_h^{n+1}) - I_3(u_h^n)|}{\int_0^1 [(u_h^{n+1})_x]^2\, dx} < TOL_2 \tag{4.3}$$

where TOL_2 is a small parameter. In the results to be presented, the value $TOL_2 = 1 \cdot 10^{-5}$ was used. If (4.3) is not satisfied, then k is cut in half and the process is repeated. The denominator in (4.3) is a convenient normalization factor.

4.3 Numerical Solutions with Grid Refinement. The experiment discussed in Section 3 to simulate the solitary-wave solution with large initial data was repeated using (4.2) and (4.3) for spatial and temporal grid refinement, respectively. These experiments showed that the solution was unstable; such instabilities being arguably precipitated by roundoff and truncation errors. To hasten the development of the instability, it was found convenient to use as initial data

$$u^0(x) = 1.01A\, sech^{2/p}[B(x - x_0)]$$

are added, *NSPLIT*
mple, with *NSPLIT*
PLIT increases to 2,
5], $h^* = 1/400$, and
that the peak of the

te conservation law

, ..., J.

me arbitrarily small
ur particular choice
on Ω^*. Specifically,
eased. At each step,

d h^* if

allow for new nodes

justed in an attempt
nt is defined by

t of the value of t.
size k. It is accepted

, the value TOL_2 =
e process is repeated.

discussed in Section
repeated using (4.2)
These experiments
rguably precipitated
he instability, it was

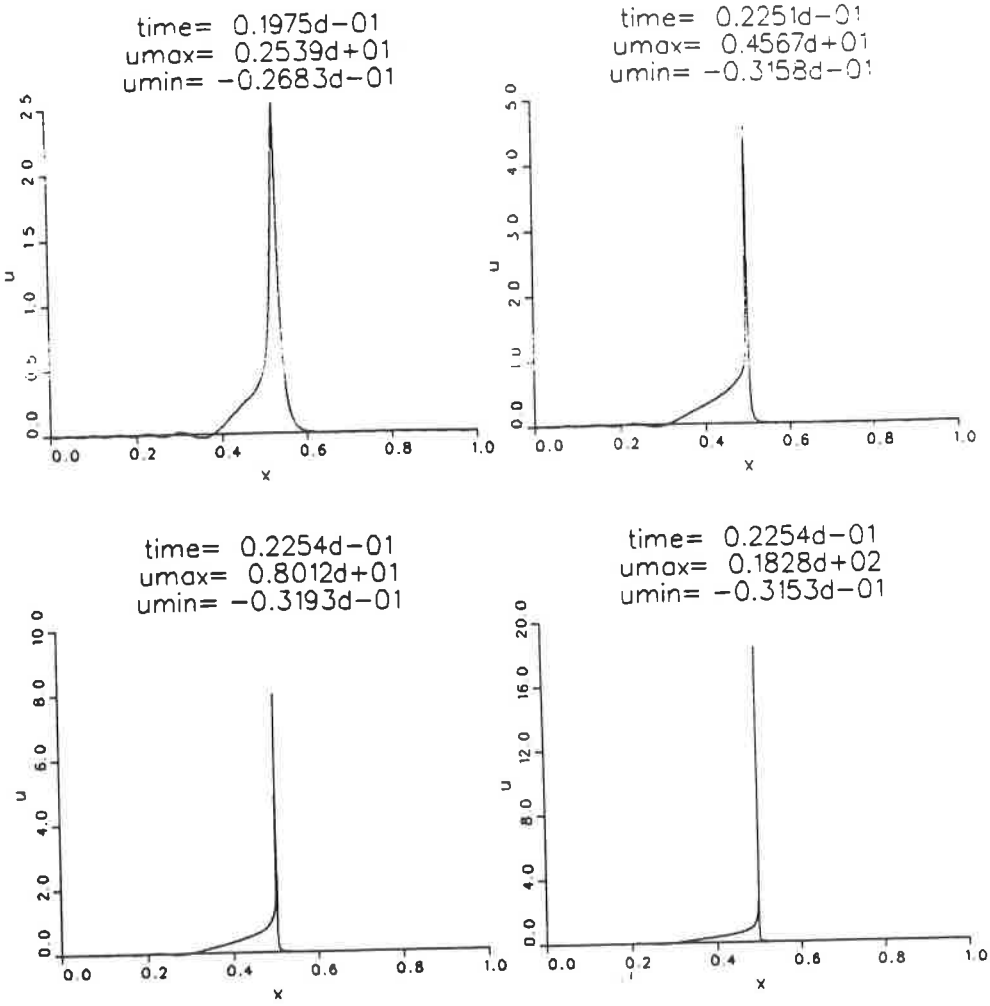

Figure 3. Numerical simulation of a solitary-wave solution with grid refinement, u-axis scaled.

with $A = 2.0, p = 5, \epsilon = 5 \cdot 10^{-4}$, and $x_0 = 1/2$. Again, use was made of the 2-stage Gauss-Legendre method with cubic splines ($q = 2, r = 4$). The initial mesh parameters were $h = 1/192$ and $k = 1/1000$. The graphs in Figure 3 illustrate the growth in the peak of the solution. The plots given are at *NSPLIT*= 2, 4, 6, 9. Note that as the peak (*umax* in the plots) significantly increases, we are forced to rescale the vertical axis in order to plot the entire solution. This has the effect of making the numerical solution u_h^n appear to be zero almost everywhere except at the peak, which, due to the translations, is kept near the midpoint $x = 1/2$. Indeed, more plots of this type would convey very little information.

In order to examine the nature of the solution near the peak as the peak continues to grow, one needs to rescale the horizontal axis. Recall that Ω^* is the region of finest grids with center at $x = .5$ and define $\Omega^0 = \Omega^* - 0.5$. In Figure 4 the solution is translated by 0.5 so that the peak is near 0 and then graphed using Ω^0 as the x-axis. The plots given

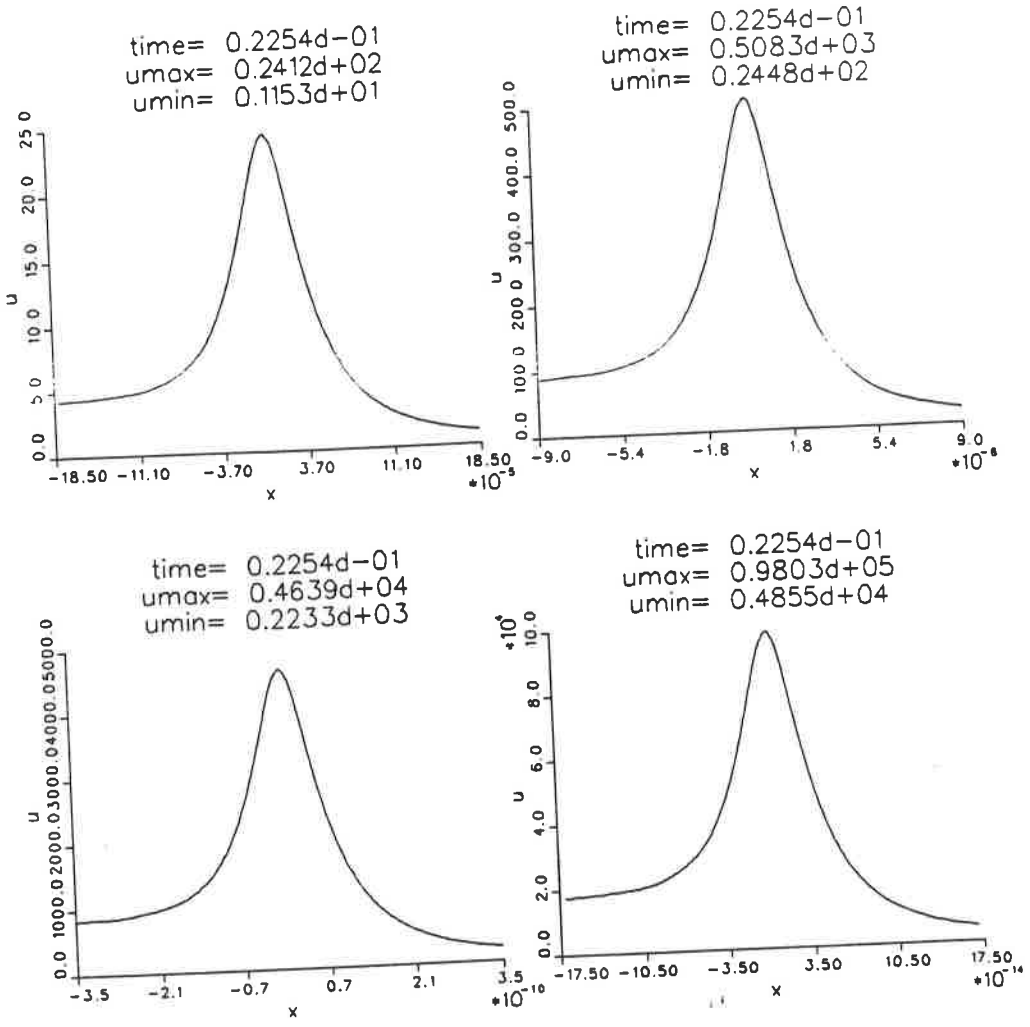

Figure 4. Numerical simulation of a solitary-wave solution with grid refinement, both axes scaled.

are with $NSPLIT = 10, 21, 29, 40$. By the final plot, the spatial and temporal mesh sizes have decreased to approximately $h \approx 10^{-14}$ and $k \approx 10^{-38}$ respectively. Our code is able to follow the peak until it reaches approximately 200,000 while maintaining a smooth profile everywhere including Ω^*. The graphs in Figure 4 suggest that instabilities of solitary-waves can lead to blowup of solutions in L^∞ in finite time.

REFERENCES

1. T. Kato, *On the Cauchy problem for the (generalized) Korteweg-de Vries equation*, Studies in Appl. Math., Advances in Mathematics Supplementary Studies, Academic Press, NY **8** (1983), 93-130.

2. J.L. Bona and R. Smith, *The initial-value problem for the Korteweg-de Vries equation*, Philos. Trans. Roy. Soc. London Ser. A **278** (1975), 555-604.

3. J.L. Bona, P.E. Souganidis and W.A. Strauss, *Stability and instability of solitary waves of KdV type*, Proc. Royal Soc. London **A 411** (1987), 395-412.

4. J.L.Bona, V.A. Dougalis, O.A. Karakashian and W.R. McKinney, *Conservative high order schemes for the Generalized Korteweg-de Vries equation*, submitted.

5. J.L.Bona, V.A. Dougalis and O.A. Karakashian, *Fully-discrete Galerkin methods for the Korteweg-de Vries equation*, Comp. & Maths. with Appls. **12A No. 7** (1986), 859-884.

6. G.A. Baker, V.A. Dougalis and O.A. Karakashian, *Convergence of Galerkin approximations for the Korteweg-de Vries equation*, Math. Comp. **40** (1983), 419-433.

7. K. Dekker and J.G. Verwer, *Stability of Runge-Kutta methods for stiff nonlinear differential equations, CWI monographs*, North Holland, Amsterdam (1984).

8. O.A. Karakashian and W.R. McKinney, *On optimal high order in time approximations for the Korteweg-de Vries equation*, Math. Comp., to appear.

54d-01
83d+03
48d+02

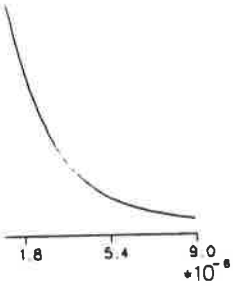

254d-01
303d+05
355d+04

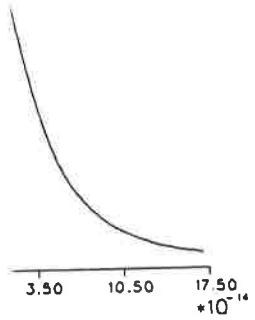

ıve

temporal mesh sizes
vely. Our code is able
ıaintaining a smooth
t that instabilities of
:.

'ries equation, Studies in
mic Press, NY 8 (1983),

:e Vries equation, Philos.